LBNL-57492

arXiv:cond-mat/0601084v1 [cond-mat.str-el] 5 Jan 2006

Self-contained Kondo effect in single molecules

C. H. Booth,[1] M. D. Walter,[1] M. Daniel,[1] W. W. Lukens,[1] and R. A. Andersen[1, 2]

[1]*Chemical Sciences Division, Lawrence Berkeley National Laboratory, Berkeley, California 94720, USA*
[2]*Department of Chemistry, University of California, Berkeley, California 94720, USA*

(Dated: Phys. Rev. Lett., in press as of Oct. 28, 2005)

Kondo coupling of f and conduction electrons is a common feature of f-electron intermetallics. Similar effects should occur in carbon ring systems (metallocenes). Evidence for Kondo coupling in $Ce(C_8H_8)_2$ (cerocene) and the ytterbocene $Cp^*{}_2Yb(bipy)$ is reported from magnetic susceptibility and $L_{\rm III}$-edge x-ray absorption spectroscopy. These well-defined systems provide a new way to study the Kondo effect on the nanoscale, should generate insight into the Anderson Lattice problem, and indicate the importance of this often-ignored contribution to bonding in organometallics.

PACS numbers: 75.20.Hr, 33.15.-e 61.10.Ht, 71.27.+a

Investigations into the Kondo effect, whereby a local magnetic moment spin-polarizes local conduction electrons forming a magnetic singlet, has recently broadened from the realm of understanding heavy-fermion, mixed valent and other related intermetallic alloys, to the study of transport and magnetic properties of quantum dots [1, 2], carbon nanotubes [3, 4], intermetallic nanoparticles [5], and even single-molecule transistors [6, 7]. Self-contained systems, where the conduction electrons are intrinsic rather than injected, are difficult to obtain experimentally, although theoretical attention has recently focused on magnetic impurities in $\lesssim$1 nm metallic nanoparticles [8, 9, 10]. Similar interactions should occur in metal-carbon ring molecules (metallocenes) where the π-bonded electrons are delocalized [11]. Here, we describe experimental evidence that the Kondo effect occurs in single molecules (Fig. 1) of cerocene [Ce(COT)$_2$, where COT = cyclooctatetraene = C_8H_8] and the ytterbocene $Cp^*{}_2Yb(bipy)$ [Cp* = pentamethylcyclopentadienyl = C_5Me_5, bipy = 2,2′-bipyridyl = $(NC_5H_4)_2$] from both temperature-dependent magnetic susceptibility $\chi(T)$ and f-occupancy measurements using rare-earth $L_{\rm III}$-edge x-ray absorption near-edge spectroscopy (XANES). These results not only provide a new arena for studying the Kondo effect on the nanoscale, but also indicate the importance of this often-ignored contribution to bonding in organometallics and provide insight into the more general Anderson Lattice problem.

The main difference between the Kondo effect in a bulk system and a nanoparticle is due to quantum confinement, where the system is small enough that the conduction band is no longer continuous, instead forming a set of discrete states with energy gap Δ [8, 9, 10]. This problem is essentially a particle-in-a-box coupling to a magnetic impurity, and so has been dubbed a "Kondo box" [8]. In a conventional metallic lanthanide Kondo system with a continuous density of states at the Fermi level, calculations show that $\chi(T)$ approaches a constant χ_0 as $T \to 0$, and for magnetic quantum numbers $J > 1$, it goes through a maximum near $T \approx \frac{1}{4}T_{\rm K}$ [12]. In a nanoparticle for $T > \Delta$, the system will behave similarly to the bulk, continuously filling the high-T triplet state from the low-T singlet state, that is, changing from a reduced $\chi(T)$ at low T to a Curie-Weiss $\chi(T)$ at high T. Both nanoparticle and bulk systems are in a multiconfigurational, quantum mechanically mixed ground state of the n_f=0 and 1 states, with the f-electron (for Ce) or f-hole (for Yb) occupancy n_f in the range of ~0.7-1.0. For $T_{\rm K} \gtrsim 1000$ K, n_f should change little with T [13].

The situation changes for $\chi(T)$ at $T < \Delta$, although exactly how probably depends on the details of the system in question. One possibility is that $\chi(T) \to 0$ as $T \to 0$ and is exponentially activated as T approaches Δ [9, 10], similarly to a Kondo insulator [14]. Implicit in this calculation is that the Landé g-values of the f-ion and conduction electrons are the same. If one instead allows different g's (eg., g=6/7 for Ce and 2 for conjugated π electrons), one should obtain a T-independent, van Vleck paramagnetic state as $T \to 0$ [15]. Another possibility [8] is that the Kondo resonance survives even up to $\Delta/T_{\rm K} \sim 5$, and therefore a continuous density of states exists. If the resonance width is proportional to $T_{\rm K}$ as in the bulk model, one expects a partial filling of the states above Δ, and $\chi(T) \to \chi_0$ at low T. Thus, even in a nanoparticle, one may obtain qualitatively similar behavior in $\chi(T)$ to a bulk system. A molecular Kondo system should allow exploring these issues in a

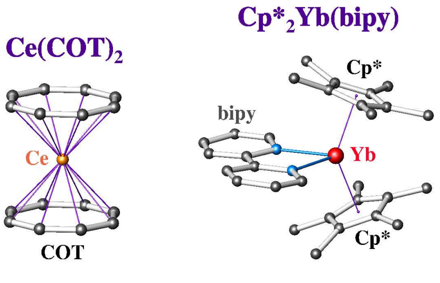

FIG. 1: The crystal structure of cerocene is shown on the left, while the structure of $Cp^*{}_2Yb(bipy)$ is shown on the right. Hydrogens atoms are not shown.

well-defined, monodispersed system that is small enough to create large energy gaps.

We begin by investigating cerocene and comparing these results to previous theoretical predictions [11, 16, 17]. The high measured T_K prevents the observation of any T-dependent effects. Consequently, Cp*$_2$Yb(bipy) is investigated as an example of a molecule with a lower T_K where clear T-dependent effects are observed. Deviations between a conventional (bulk) Kondo model and these data are noted, and possible explanations are discussed.

Cerocene (Fig. 1) might seem like a strange place to look for Kondo interactions, because the required local moment would be due to partial occupancy of the Ce f-orbital. Since its initial synthesis nearly 30 years ago [19], Ce in cerocene was believed to have a tetravalent, f^0 ground state. Atomic radii arguments [20] and cerocene's apparent diamagnetism are consistent with the nominal Ce(IV) assignment, and gas phase photoelectron spectra [21] show no obvious signs of f-electron ionization. However, Dolg, Fulde, and co-authors [11, 16, 17] later postulated that the ground state of cerium is close to Ce(III) f^1 with an admixture of Ce(IV) f^0 character. In this picture, strong correlations between the C π-electrons and the Ce f-electrons produce a singlet ground state, as in the Kondo interaction. Multiconfiguration interaction calculations indicate that this f(Ce)/p(C) coupling is very strong, leading to a mixed-valent ground state with an f-occupancy of $n_f \approx 0.80$ and a $T_K \approx 11,600$ K. The only experimental evidence supporting this conclusion are Ce K-edge XANES spectra [22] of the substituted cerocenes Ce(η^8-1,4-(TMS)$_2$C$_8$H$_6$)$_2$ and Ce(η^8-1,3,6-(TMS)$_3$C$_8$H$_5$)$_2$ indicating that the K-edge position is similar to that from various Ce(III) model compounds.

In order to enhance previous studies of the physical properties of cerocene, a better synthesis was developed as the literature synthesis only yields small amounts of product, making purification difficult. High yields were obtained by oxidizing the anion, [Ce(COT)$_2$]$^-$ to cerocene using ferrocenium salts or para-quinone.

Since the metallocenes are extremely sensitive to air, special sample holders for both the $\chi(T)$ and the XANES measurements are used. Susceptibility samples were sealed into 3 mm-diameter quartz tubes, and held in place with a small amount of quartz wool. The total background was typically $\sim 2 \times 10^{-5}$ emu (eg. ∼30% of the signal at 300 K for cerocene). XANES holders consist of an aluminum body with machined slots. The samples (typically about 5 mg of ground powder) were mixed with boron nitride and packed into the slots. Pinhole-free 0.001" aluminum windows were affixed to the holder with a lead-wire seal. This design allows measurements between 10-600 K while maintaining isolation from air.

Magnetic susceptibility was measured with a Quantum Design superconducting quantum interference device (SQUID) magnetometer. Small impurity contributions (so-called "Curie tails") are removed. For cerocene, a fit to a Curie-Weiss form plus a constant yields an impurity contribution with Curie constant C_J=0.00167 emu·K/mol and Weiss temperature $\Theta_{CW} = -9.1$ K, corresponding to ∼0.2% J=5/2 impurity. The diamagnetic contribution from the complex has also been removed within 1% using Pascal corrections [18]. For example, while the cerocene molecule is diamagnetic with $\chi(T) = -(2.7 \pm 0.2) \times 10^{-5}$ emu/mol, the Pascal constants indicate that the (COT)$_2$ portion is $\chi(T) = -1.67 \times 10^{-4}$ emu/mol. The remaining cerium ion susceptibility is therefore positive with a similar magnitude.

Figure 2 shows the cerium contribution to $\chi(T)$ for cerocene after background corrections both with and without the impurity contribution. The cerium ion displays characteristics of T-independent paramagnetism (TIP) with $\chi(T) = (1.4 \pm 0.2) \times 10^{-4}$ emu/mol. Estimating of T_K from this result depends on whether one assumes a

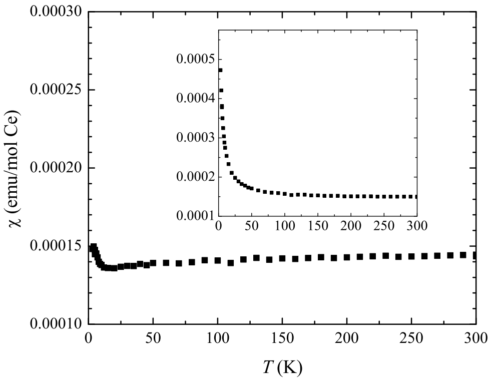

FIG. 2: Cerium contribution to the magnetic susceptibility of cerocene, Ce(COT)$_2$. The diamagnetic contribution from the (COT)$_2$ has also been removed using Pascal constants [18]. Inset: data including a small magnetic impurity (∼0.2% of a J=5/2 impurity), removed in data from main panel.

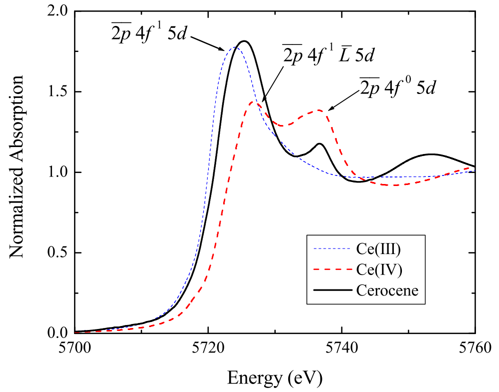

FIG. 3: Ce L_{III} XANES of cerocene, and Ce(III) and Ce(IV) references (see text). Final state configurations for the references, as determined in the literature, are indicated.

continuum of states, as discussed earlier. If the TIP is due to van Vleck paramagnetism, we expect $\chi_0 \sim 1/T_{\mathrm{K}}$, since T_{K} is the difference in energy between the singlet and triplet states. However, we don't know the proportionality constant without a more detailed calculation. If we assume the Kondo resonance generates a continuum of states, one can use the Coqblin-Schriefer model to obtain $T_{\mathrm{K}} = \frac{2J+1}{2\pi}\frac{C_J}{\chi_0}$ [12] where J=5/2, $T_{\mathrm{K}} \approx 0.770/\chi_0$=5,500 K from these data, in rough agreement with the value of 11,600 K from the calculation [17].

XANES data were collected on BL 11-2 at the Stanford Synchrotron Radiation Laboratory (SSRL) using a Rh-coated mirror to reject energies $\gtrsim$ 9 keV. The double Si(220) monochromator crystals were detuned for further rejection. Samples were placed in a LHe-flow cryostat. Figure 3 shows the XANES data for cerocene and two reference standards: a Ce(III) standard, Ce[N(Si(CH$_3$)$_3$)$_2$]$_3$, and a Ce(IV) standard, Ce[5,7,12,14-Me$_4$-2,3:9,10-dibenzo[14]hexaenato(2-)N$_4$]$_2$ = Ce(tmtaa)$_2$. It is important to note that formally Ce(IV) systems generally are strongly mixed valent [23], as first observed in CeO$_2$ and later in other formally Ce(IV) systems [24]. The Ce(III) standard has XANES typical of the L_{III} edge of a rare earth in a single valence configuration, displaying a sharp resonance just above the threshold, followed by comparatively small oscillations due to elastic scattering of the photoelectron by neighboring atoms. The final state includes the core hole ($\overline{2p_{3/2}}$) and the excited state 5d, that is, $\overline{2p_{3/2}}f^1 5d$. Like CeO$_2$, the initial state of the Ce(IV) standard Ce(tmtaa)$_2$ is a superposition of states, close to $\frac{1}{2}|f^0> + \frac{1}{2}|f^1\overline{L}>$, where $\overline{L}$ indicates a ligand hole. The interaction of the $\overline{2p_{3/2}}$ core hole with the f orbital splits the final state into $\overline{2p_{3/2}}f^0 5d$ and $\overline{2p_{3/2}}f^1\overline{L}5d$ configurations [23]. This splitting is clearly visible in the Ce L_{III}-edge spectra of cerocene and allows a more precise estimate of the cerium valence than the previous Ce K-edge work. Indeed, this spectrum unequivocally shows that while cerium in cerocene is much closer to Ce(III) than the Ce(IV) model compound in agreement with the previous measurement [22], it also displays a pronounced feature indicative of an f^0 component and therefore is mixed valent. These data have been fit with a combination of an integrated pseudo-Voigt to simulate the main edge and other pseudo-Voigts to model the resonance features. We estimate $n_f = 0.89 \pm 0.03$ from these fits. We observe no change in n_f with T until the system decomposes above ∼565 K. These data compare favorably with the value of $n_f = 0.80$ obtained in the calculations [17]. Moreover, the measurement is consistent with a strongly mixed valent system as expected from the high predicted value of T_{K} [13].

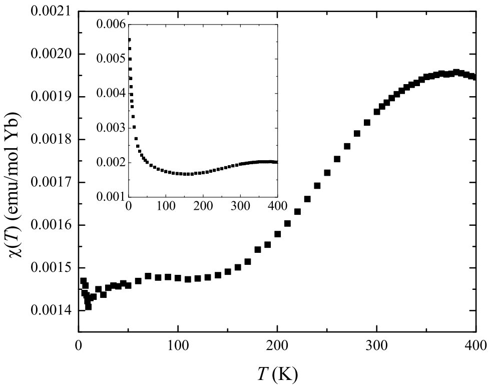

FIG. 4: Ytterbium contribution to the magnetic susceptibility of Cp*$_2$Yb(bipy). Inset: data including impurity (∼1% of a J=7/2 impurity), removed in data from main panel.

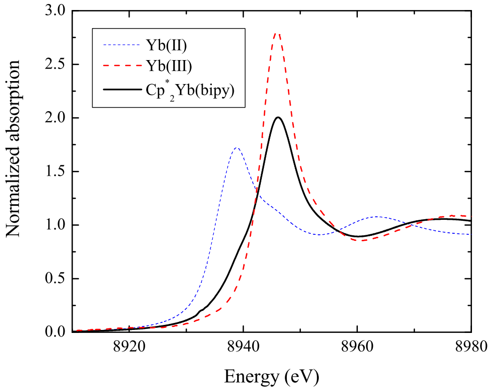

FIG. 5: Yb L_{III} XANES for Cp*$_2$Yb(bipy), and Yb(II) and Yb(III) references (see text).

Next we study how the ground state and T dependence evolve in a system with a lower T_{K}, the ytterbocene Cp*$_2$Yb(bipy) (see Fig. 1), where Yb is regarded as the hole analogue to Ce, and similar magnetic behavior is expected. In contrast to cerocene, the f-electrons couple with the bipy π-bonded electrons, since f-orbital overlap with π-orbitals of the canted Cp*'s is small.

Samples of Cp*$_2$Yb(bipy), as well as Cp*$_2$Yb(OEt)$_2$ and Cp*$_2$Yb(bipy)I as Yb(II) and Yb(III) reference compounds, respectively, were synthesized and crystal structures obtained using previously discussed methods [25]. Magnetic susceptibility data for the ytterbium contribution to Cp*$_2$Yb(bipy) are shown in Fig. 4 after the Pascal corrections, with and without the impurity contribution removed. The impurity contribution in the Cp*$_2$Yb(bipy) data is slightly non-Curie-Weiss-like at low T, that is, $1/\chi(T)$ is not linear with T. This nonlinearity is observed in other ytterbocenes synthesized in our lab. We overcome this difficulty by modeling the impurity contribution with data from the non-magnetic Cp*$_2$Yb(II)(py)$_2$ system, where the impurity contribution corresponds to less than ∼0.5% of a J=7/2 impurity. The total impurity in the Cp*$_2$Yb(bipy) data is roughly twice as large.

These $\chi(T)$ data show significant T dependence in $\chi(T)$, with clear evidence of both TIP at low T with $\chi_0 = (1.46\pm0.02)\times10^{-3}$ emu/mol and a strong maximum $\chi_{\max}$ in the susceptibility at $T(\chi_{\max}) \approx 380$ K. Yb $L_{\rm III}$-edge XANES data (Fig. 5) are consistent with the $\chi(T)$ data. In this case, the f^{14} configuration is non-magnetic, and the estimated f-hole occupancy n_f=0.07, 0.80, and 1.00±0.03 for the Cp$^*{}_2$Yb(II)(OEt)$_2$, Cp$^*{}_2$Yb(bipy), and Cp$^*{}_2$Yb(bipy)I, respectively. No change in these values has been observed from 10 K up to the T at which the samples decompose, above ~ 400 K.

Although there have been no detailed theoretical calculations on Cp$^*{}_2$Yb(bipy), the T dependence and the observed $\chi_{\max}$ in addition to the measured mixed valence make a strong case for Kondo-like interactions. In this instance, assuming a continuum of states and J=7/2, we estimate $T_{\rm K}$ from $T_{\rm K} = 3.27/\chi_0 = 2240$ K and $T_{\rm K} = 4.4T(\chi_{\max}) = 1670$ K; these estimates are in reasonable agreement. Moreover, we measure $\chi_{\max}/\chi_0 = 1.34$, compared to the J=7/2 calculation of 1.22 [12] , also in reasonable agreement especially when one considers that $\chi_{\max}/\chi_0$ grows with increasing mixed valence in the non-crossing approximation (NCA) [13]. If one instead assumes discrete states and a van Vleck TIP as $T \to 0$, the observed T-dependence would be due to activation to the triplet level. Since T_K estimates from both χ_0 and $T(\chi_{\max})$ assuming a continuum of states are similar, we tend to favor the idea that a Kondo resonance induces bulk-like behavior, but the discrete-states, van Vleck model cannot be ruled out from these data.

Evidence of activated behavior in $\chi(T)$ is not observed for either the cerocene or ytterbocene molecules, implying that within the continuum of states picture Δ is $\lesssim 0.2$ eV, and that a lower $T_{\rm K}$ is still required to observe the predicted activated behavior. It is important to point out that the enhanced $\chi_{\max}/\chi_0$ ratio may be due to a size-induced suppression of χ_0 as $T_{\rm K}$ approaches Δ, also accounting for the higher estimate of $T_{\rm K}$ from χ_0 compared to that from $T(\chi_{\max})$. In fact, our early results on some related molecules show that $\chi_{\max}/\chi_0$ grows as $n_f \to 1$, opposite to that expected from calculations in the NCA [13]. Another important possibility is that the number of electrons available for screening the f-hole moment is close to unity. In that case, the screening cloud could be over or under damped and the susceptibility can approach the high-T local moment state either more quickly or more slowly with T than in a single impurity model [26]. This issue therefore directly links these materials to current topics in understanding the Anderson Lattice.

In summary, the Kondo model has been used to understand the electronic and magnetic behavior of cerocene Ce(COT)$_2$ and the ytterbocene Cp$^*{}_2$Yb(bipy). The experimental results for cerocene are in close agreement with theory, both from pseudopotential calculations [17] and bulk Kondo calculations. In particular, $\chi(T)$ of cerocene is T independent, consistent with the high value of $T_{\rm K}$, and the valence is close to Ce(III) with some Ce(IV) character. Data on Cp$^*{}_2$Yb(bipy) are qualitatively similar, except that $T_{\rm K}$ is low enough that $\chi(T)$ is T-dependent, showing TIP susceptibility below $\sim$150 K and a clear maximum at about 380 K, consistent with the measured valence within the Kondo model. Finally, deviations from the standard Kondo picture exist, possibly due to size effects.

We thank E. D. Bauer, D. L. Cox, M. Crommie, J. M. Lawrence, J. L. Sarrao and P. Schlottmann for many useful discussions. This work was supported by the Director, Office of Science, Office of Basic Energy Sciences (OBES), Chemical Sciences, Geosciences and Biosciences Division, U.S. Department of Energy (DOE) under Contract No. AC03-76SF00098. XANES data were collected at the SSRL, a national user facility operated by Stanford University of behalf of the DOE/OBES.

[1] D. Goldhaber-Gordon *et al.*, Nature **391**, 156 (1998).
[2] S. M. Cronenwett, T. H. Oosterkamp, and L. P. Kouwenhoven, Science **281**, 540 (1998).
[3] M. R. Buitelaar *et al.*, Phys. Rev. Lett. **88**, 156801 (2002).
[4] J. Nygård, D. H. Cobden, and P. E. Lindelof, Nature **408**, 342 (2000).
[5] Y. Y. Chen *et al.*, Phys. Rev. Lett. **84**, 4990 (2000).
[6] J. Park *et al.*, Nature **417**, 722 (2002).
[7] W. Liang *et al.*, Nature **417**, 725 (2002).
[8] W. B. Thimm, J. Kroha, and J. von Delft, Phys. Rev. Lett. **82**, 2143 (1999).
[9] P. Schlottmann, Phys. Rev. B **65**, 024420 (2002).
[10] P. Schlottmann, Phys. Rev. B **65**, 024431 (2002).
[11] C.-S. Neumann and P. Fulde, Z. Phys. B **74**, 277 (1989).
[12] V. T. Rajan, Phys. Rev. Lett. **51**, 308 (1983).
[13] N. E. Bickers, D. L. Cox, and J. W. Wilkins, Phys. Rev. B **36**, 2036 (1987).
[14] P. Riseborough, Adv. Phys. **49**, 257 (2000).
[15] P. Schlottmann, private communication.
[16] M. Dolg *et al.*, J. Chem. Phys. **94**, 3011 (1991).
[17] M. Dolg *et al.*, Chem. Phys. **195**, 71 (1995).
[18] L. N. Mulay and E. A. Boudreaux, *Theory and Application of Molecular Diamagnetism* (Wiley-Interscience, New York, 1976).
[19] A. Greco, S. Cesca, and G. Bertolini, J. Organomet. Chem. **113**, 321 (1976).
[20] K. N. Raymond and C. W. Eigenbrot, Acc. Chem. Res. **13**, 276 (1980).
[21] A. Streitwieser *et al.*, J. Am. Chem. Soc. **107**, 7786 (1985).
[22] N. M. Edelstein *et al.*, J. Am. Chem. Soc. **118**, 13115 (1996).
[23] A. Kotani, T. Jo, and J. C. Parlebas, Adv. Phys. **37**, 37 (1988).
[24] G. Kaindl *et al.*, Phys. Rev. B **38**, R10174 (1988).
[25] M. Schultz *et al.*, Organometallics **21**, 460 (2002).
[26] A. N. Tahvildar-Zadeh, M. Jarrell, and J. K. Freericks, Phys. Rev. B **55**, R3332 (1997).